

Received July 3, 2020, accepted July 18, 2020, date of publication July 28, 2020, date of current version August 7, 2020.

Digital Object Identifier 10.1109/ACCESS.2020.3012462

# Robust Control for Switched Systems With Unmatched Uncertainties Based on Switched Robust Integral Sliding Mode

XIAOYU ZHANG<sup>1</sup>, (Senior Member, IEEE), LINGFEI XIAO<sup>2</sup>, AND HAIFEN LI<sup>1</sup>

<sup>1</sup>North China Institute of Science and Technology, Beijing 101601, China

<sup>2</sup>College of Energy and Power Engineering, Nanjing University of Aeronautics and Astronautics, Nanjing 210016, China

Corresponding author: Xiaoyu Zhang (xyzhang@ieee.org)

This work was supported in part by the National Natural Science Foundation of China under Grant 61304024 and Grant 51876089, and in part by the Fundamental Research Funds for the Central Universities under Grant 3142016022 and Grant 3142018048.

**ABSTRACT** This paper proposes a robust control design based on a new switched robust integral sliding mode (SRISM) for switched systems with unmatched uncertainties. The SRISM is a sliding surface consisting of multiple sliding modes of subsystems and is robust with respect to the structural decomposed unmatched uncertainties. Each sliding mode of the subsystem can suppress the unmatched uncertainties. Their parameters are given by the conditions of linear matrix inequalities (LMIs), and their reachabilities are guaranteed by the sliding mode controllers. Finally, numerical and application simulation results for an inverted pendulum swing-up control are provided to illustrate the validity of the robust control design.

**INDEX TERMS** Switched systems, unmatched uncertainty, sliding mode control, robustness, integral sliding mode.

## I. INTRODUCTION

A switched system (SS) is a complicated dynamic system shaped by a number of subsystems. It is controlled not only by the subsystem controllers, but also by the logical rules that create the switching sequence. An SS represents many control processes in practice [1], [2], such as the processes in mechanical systems, power systems, traffic control systems and industrial processes. Due to the switching or jump characteristic of all kinds of SSs, many attentions have been attracted about their complicated moving mechanism and problems. For some recent interesting examples, there are the output feedback control design for Markov jump repeated scalar nonlinear systems [3], the reachable set estimation for Markov jump inertial neural networks with time-varying delay [4], and the filtering problem for discrete-time switched singular systems under the circumstance of sensor failures [5].

Sliding mode control (SMC) is an excellent robust control strategy for an SS that has the obvious advantage of compensation for the matched uncertainties/perturbations [6], [7]. During recent years, SMC synthesis for SS was extensively

investigated [8]–[18]. Among these SMC designs, the integral sliding mode (ISM) method ([19], [20]) is an efficient approach for increasing the robustness. The ISM method is advantageous due to its elimination of the reaching phase that is not robust with respect to uncertainty and disturbance. As a result, throughout the entire control process, the robustness of the system is confirmed from the initial point in time. The SMC design based on the ISM method for SS has attracted much attention. For example, [21] presented the robust integral sliding mode control design for a class of uncertain switched nonlinear systems and a similar robust  $H_\infty$  integral sliding mode control [22]. The ISM control synthesis scheme under switching laws with an average dwell time was developed. However, in some cases, the switching frequency of the SMC should be infinite so that the sliding motion can be guaranteed. Therefore, a typical problem encountered when using this approach is that the state of the closed-loop system may jump under the sliding mode because the ISM contains switches with the switching signal [23]. A similar point was also discussed by [24] for the two structures employed by [21], [22]. One structure is the controller structural switching around a pre-specified switching surface, and the other one is the system structural switching with an average dwell time. This kind of sliding surface may result in repetitive

The associate editor coordinating the review of this manuscript and approving it for publication was Hao Shen<sup>1</sup>.

jumps of the state trajectories between the sliding surface and hence may give rise to instability [6]. Therefore, [25] presented the common robust integral sliding mode (CRISM) method under arbitrary switching rules to avoid the possible jumping problem.

Recently, the ISM method has been successfully applied to the uncertain SS to compensate exactly the matched uncertainties or perturbations. For example, Kchaou and Ahmadi extended an adaptive SMC design based on the switched integral sliding mode (SISM) for a class of uncertain switched descriptor systems with state delay and nonlinear input [26]. Ferrara *et al.* proposed a switching structure scheme for the motion control of industrial robot manipulators [27]. However, these ISMs still display the jump problem of the system state during the switching because this method is essentially the same as the aforementioned approaches. Galván-Guerra and Fridman proposed another switched integral sliding mode design [28] that differs from these ISM functions. This new kind of SISM is formed by the same switching rules that govern the SS under consideration, and makes the system dynamic is in the sliding mode at every switching time. Therefore, this SISM approach allows to compensate theoretically the matched uncertainties or perturbations just after the initial time instant even in the presence of switchings. It can ensure that the sliding mode function value keeps zero at every switching time instant and the system state does not need jumping to keep running on the sliding surface. Consequently, they used this developed SISM method to expand the continuous output integral sliding mode robustification for SS with state-dependent location transitions and dwell time [29], [30] and applied this SISM method to the robustification problem of self-oscillations [31], [32]. However, even though this SISM is an excellent approach, it has the disadvantage that the unmatched uncertainty or disturbance may only be minimized but not rejected.

Inspired by this kind of SISM [28]–[32], this paper presents a switched robust integral sliding mode (SRISM) design for the switched system with unmatched uncertainties. First, a kind of sliding surface with multiple sliding modes is proposed that consists of the robust integral sliding modes of the subsystems. The robust integral sliding mode (RISM) of every subsystem can reject the structured unmatched uncertainties. Then, the common Lyapunov function method and the switching rule stabilization method used to guarantee system stability in sliding mode are given. The SS will be robustly stable when running on a sliding surface with no state jumping among the different sliding modes. Finally, the SMC will be devised. and the reachability of the sliding modes will be analyzed.

The main contribution of this paper is to provide a switched robust integral sliding mode scheme for the SS with unmatched uncertainties that is different from the CRISM method in [25]. The difference lies in that the SRISM design presented in this paper is a kind of the switched integral sliding mode (SISM) surface for which the parameters are

switched following the switching signal, whereas the CRISM design presented in [25], [33] has no switched parameters or sliding mode switching. In the design method of the CRISM [25], the parameters of the CRISM have to satisfy the similar LMIs conditions from all of the subsystems. Contrarily, in the SRISM design presented by this paper, the parameters of the SRISM may be switched following the switching signal. Therefore, the parameters of the SRISM are easier to satisfy the LMIs conditions. This leads to the presented SRISM method has the more relaxed conditions.

The rest of the paper is organized as follows. Section II states the problem formulation. Section III gives the definition of the sliding surface with multiple sliding modes, and the design of the sliding modes with the stability analysis. Then, the reachabilities of the sliding modes are proved by the SMC controller design in Section 4. Numerical and application simulations are described in Section 5. Finally, Section 6 presents a brief conclusion of this paper.

## II. PROBLEM FORMULATION

Consider the following uncertain switched system

$$\dot{x}(t) = (A_\sigma + \Delta A_\sigma)x(t) + (B_\sigma + \Delta B_\sigma)[u(t) + \omega_\sigma(t)], \quad (1)$$

where  $x(t) \in \mathbb{R}^n$  is the system state vector,  $u(t) \in \mathbb{R}^m$  is the control input,  $\Delta A_\sigma$  and  $\Delta B_\sigma$  are the uncertainties of the parameters,  $\omega_\sigma(t)$  is the bounded exogenous disturbance outside the boundary, and  $\sigma(t) : \mathbb{R} \rightarrow \mathbb{N} \cong \{1, 2, \dots, N\}$  is a piecewise constant function of the time  $t$ , also referred to as the switching signal (rule). Then, we define a switching sequence:

$$Q := x_{t_0}; (i_0, t_0), (i_1, t_1), \dots, (i_k, t_k), \dots, \forall i_k \in \mathbb{N}, k \in \mathbb{Z}^+$$

where  $x_{t_0}$  is the state value at the initial time  $t_0$ . Namely, the  $i_k$ -th subsystem operates when  $t \in [t_k, t_{k+1})$ .

For the switching signal  $\sigma(t) = i$ ,  $i \in \mathbb{N}$ , the  $i$ -th subsystem matrices are denoted as:

$$A_\sigma \doteq A_i, B_\sigma \doteq B_i, \Delta A_\sigma \doteq \Delta A_i, \Delta B_\sigma \doteq \Delta B_i, \omega_\sigma(t) \doteq \omega_i(t).$$

Accordingly, for the  $k$ -th switching, when  $t_k \leq t < t_{k+1}$ , we can set  $\sigma(t) = i$ , i.e.,  $i_k = i \in \mathbb{N}$ . As a result, the system (1) can be described as:

$$\dot{x}(t) = (A_i + \Delta A_i)x(t) + (B_i + \Delta B_i)[u(t) + \omega_i(t)]. \quad (2)$$

The following assumptions are satisfied and the lemmas described below are used in this work.

*Assumption 1:*  $(A_i, B_i)$  is stabilizable and  $B_i$  is required to be full column rank.

*Assumption 2:* The uncertainty parameters,  $\Delta A_i$  and  $\Delta B_i$ , satisfy the following relationships:

$$\Delta A_i = H_{a,i} F_{a,i}(t) E_{a,i}, \Delta B_i = H_{b,i} F_{b,i}(t) E_{b,i}, \quad (3)$$

where  $H_{a,i} \in \mathbb{R}^{n \times r_a}$ ,  $H_{b,i} \in \mathbb{R}^{n \times r_b}$ ,  $E_{a,i} \in \mathbb{R}^{r_a \times n}$  and  $E_{b,i} \in \mathbb{R}^{r_b \times m}$  are all of the known-constant matrices, and the unknown time-varying matrices  $F_{a,i}(t)$  and  $F_{b,i}(t)$  satisfy:

$$F_{a,i}^T(t) F_{a,i}(t) \leq I, F_{b,i}^T(t) F_{b,i}(t) \leq I.$$

*Assumption 3:* The bounded disturbance  $\omega_i(t)$  satisfies  $\|\omega_i(t)\| < d_i$ , in which  $d_i$  is a positive scalar parameter.

*Lemma 1:* Assuming that  $H$  and  $E$  are the matrices consisting of real constants with appropriate dimensions,  $F(t)$  satisfies  $F^T(t)F(t) \leq I$ . The following relation is true for any positive constant  $\varepsilon > 0$  [34]:

$$HF(t)E + E^T F^T(t)H^T \leq \varepsilon^{-1}HH^T + \varepsilon E^T E. \quad (4)$$

*Lemma 2:* For two matrices with appropriate dimensions,  $A$  and  $B$ , if  $A$  and  $I + BA^{-1}$  are non-singular, the following equation holds [35]:

$$(A + B)^{-1} = A^{-1} - A^{-1}(I + BA^{-1})^{-1}BA^{-1}. \quad (5)$$

The control task is to design an SMC control for guaranteeing the asymptotic stability of the switched system as described by (1),(2) with the unmatched uncertainties.

### III. SWITCHED ROBUST INTEGRAL SLIDING MODE SURFACE DESIGN

#### A. SLIDING SURFACE WITH MULTIPLE SLIDING MODES

Given the following definition of the sliding surface with multiple sliding modes for the SS (1).

*Definition 1:* The hypersurface

$$S(x, t) := \{S_{\sigma(t)}(x, t) = 0 \mid \sigma(t) \text{ follows } Q, \sigma(t) \in \mathbb{N}\} \quad (6)$$

is a sliding surface with multiple sliding modes of the SS (1) that consists of the sliding modes  $S_i(x, t), \forall i \in \mathbb{N}$  of the subsystems, and

$$S_i(x, t) = 0, \quad \text{when } \sigma(t) = i$$

along with the switching rule  $\sigma(t)$ . Namely, it is a kind of switched sliding mode (SSM).

*Remark 1:* The continuity of the sliding surface with multiple sliding modes plays a crucial role, namely the state  $x(t_k)$  will be on the next sub-sliding mode  $S_i(x(t_k), t_k) = 0$  when the switching occurs  $t = t_k$ .

*Remark 2:* The hypersurface (6) is composed of every sub-hyper plane  $S_i(x, t) = 0$  with every switching  $\sigma(t) = i$  that at the switching time  $t = t_k$  must have the interface between every two switching  $\sigma(t) = i - 1$  and  $i$ .

#### B. SLIDING MODES DESIGN OF SUBSYSTEMS

We formulate a robust integral sliding mode (RISM) as

$$S_i(x, t) = C_i[x(t) - x(t_k)] + \int_{t_k}^t (K_i - C_i A_i)x(t)dt, \quad (7)$$

in which the parameter  $C_i \in R^{m \times n}$  satisfies

$\forall i \in \mathbb{N}, \text{rank}(C_i B_i) = m$ , and

$$\exists 0 \leq \gamma_i < 1, \gamma_i \in R, \quad C_i \Delta B_i \leq \gamma_i C_i B_i, \quad (8)$$

another parameter  $K_i$  is the common-state-feedback stabilization coefficient to be designed and essentially ensures the matrix

$$\hat{A}_i = A_i - B_i(C_i B_i)^{-1}K_i, \forall i \in \mathbb{N} \quad (9)$$

is Hurwitz. The time  $t_k$  represents the time of the  $k$ -th switching  $\sigma(t) = i$ , certainly  $x(t_k)$  is the state value when the  $k$ -th switching occurs.

Based on (2), we can write

$$\dot{S}_i(x, t) = (C_i \Delta A_i + K_i)x(t) + C_i(B_i + \Delta B_i)[u(t) + \omega_i(t)].$$

According to the sliding mode control theory, when the system state reaches the sliding surface and remains there,  $S_i(t) = 0, \dot{S}_i(t) = 0$ . Thus, the equivalent control can be written as

$$u_{eq}(t) = -\omega_i(t) - [C_i(B_i + \Delta B_i)]^{-1}[C_i \Delta A_i + K_i]x(t). \quad (10)$$

By substituting (10) into (2), the following sliding mode equation can be written as:

$$\begin{aligned} \dot{x}(t) &= [A_i + \Delta A_i]x(t) - [B_i + \Delta B_i] \\ &\quad \times [C_i(B_i + \Delta B_i)]^{-1}[C_i \Delta A_i + K_i]x(t). \end{aligned}$$

Based on Lemma 2 and (8) (the design condition of the parameter  $C_i$ ), the above equation can be rewritten as:

$$\begin{aligned} \dot{x}(t) &= [A_i + \Delta A_i]x(t) - (B_i + \Delta B_i)(I - M_i) \\ &\quad \times (C_i B_i)^{-1}[K_i + C_i \Delta A_i]x(t), \end{aligned}$$

in which  $M_i \in R^{m \times m}$  and can be written as:

$$M_i = (C_i B_i)^{-1}[I + C_i \Delta B_i(C_i B_i)^{-1}]^{-1}C_i \Delta B_i. \quad (11)$$

As shown in (10),  $C_i(B_i + \Delta B_i)$  is required to be nonsingular. It can be inferred from (8) that  $C_i(B_i + \Delta B_i)$  is nonsingular and

$$\| [I + C_i \Delta B_i(C_i B_i)^{-1}]^{-1} \| \leq \frac{1}{1 - \gamma_i}. \quad (12)$$

Defining that

$$\begin{cases} H_{u,i} = B_i(C_i B_i)^{-1}, \\ \hat{C}_i = I - H_{u,i}C_i, \\ N_i = (\Delta B_i - B_i M_i - \Delta B_i M_i)(C_i B_i)^{-1}, \end{cases} \quad (13)$$

then the sliding mode equation can be rewritten as

$$\dot{x}(t) = [\hat{A}_i + \hat{C}_i \Delta A_i - N_i C_i \Delta A_i - N_i K_i]x(t), \quad (14)$$

i.e.,

$$\dot{x}(t) = \bar{A}_i x(t), \quad (15)$$

where

$$\bar{A}_i = \hat{A}_i + \hat{C}_i \Delta A_i - N_i C_i \Delta A_i - N_i K_i. \quad (16)$$

The design result of the parameter  $K_i$  for the RISM (7) is presented.

*Theorem 1:* The coefficient  $K_i$  that guarantees the Lyapunov stability of the sliding mode matrix (9) of the system (2) enables  $\hat{\mathbb{A}} = \{\hat{A}_1, \hat{A}_2, \dots, \hat{A}_N\}$  to be a robust stable matrix set in which each stable matrix  $\hat{A}_i$  has robust stability if there exists a symmetric positive definite matrix set  $P_i (P_i = P_i^T \text{ and } P_i > 0)$ , and the corresponding scalar set

$\varepsilon_i > 0$  that can satisfy the following linear matrix inequalities (LMIs):

$$\begin{bmatrix} \Theta_i & P_i \hat{C}_i H_{a,i} & \tau_{i,1} P_i H_{u,i} & \tau_{i,2} P_i H_{b,i} \\ * & -\varepsilon_i I_{r_a \times r_a} & 0 & 0 \\ * & * & -\varepsilon_i I_{m \times m} & 0 \\ * & * & * & -\varepsilon_i I_{r_b \times r_b} \end{bmatrix} < 0, \quad (17)$$

where

$$\Theta_i = P_i \hat{A}_i + \hat{A}_i^T P_i + 4\varepsilon_i E_{a,i}^T E_{a,i} + 3\varepsilon_i \bar{E}_{b,i}^T \bar{E}_{b,i}, \quad (18)$$

$$\tau_{i,1} = \text{sqrt}\left[\frac{(1 + \delta_{i,1})\delta_{i,2}}{(1 - \gamma_i)^2}\right], \quad (19)$$

$$\tau_{i,2} = \text{sqrt}\left[1 + \delta_{i,1} + \frac{(1 + \delta_{i,1})\delta_{i,2}\delta_{i,3}}{(1 - \gamma_i)^2}\right], \quad (20)$$

with

$$\begin{aligned} \bar{E}_{b,i} &= E_{b,i}(C_i B_i)^{-1} K_i, \\ \delta_{i,1} &= \lambda_{\max}[E_{b,i}(C_i B_i)^{-1} C_i H_{a,i} H_{a,i}^T C_i^T (C_i B_i)^{-T} E_{b,i}^T], \\ \delta_{i,2} &= \lambda_{\max}[C_i H_{b,i} H_{b,i}^T C_i^T], \\ \delta_{i,3} &= \lambda_{\max}[E_{b,i}(C_i B_i)^{-1} (C_i B_i)^{-T} E_{b,i}^T]. \end{aligned}$$

(Here,  $\lambda_{\max}[\cdot]$  represents the calculation of the matrix's maximum eigenvalue, i.e., the spectral norm of the symmetric matrix)

*Proof:* For each subsystem, we select its Lypunov function:

$$V_i(t) = x^T(t) P_i x(t). \quad (21)$$

According to (14), the derivative of  $V_i(t)$  with respect to the time is given by

$$\begin{aligned} \dot{V}_i(t) &= x^T(t) (\hat{A}_i^T P_i + P_i \hat{A}_i) x(t) + x^T(t) [\hat{C}_i \Delta A_i \\ &\quad - N_i C_i \Delta A_i - N_i K_i]^T P_i x(t) \\ &\quad + x^T(t) P_i [\hat{C}_i \Delta A_i - N_i C_i \Delta A_i - N_i K_i] x(t) \\ &= x^T(t) (\hat{A}_i^T P_i + P_i \hat{A}_i) x(t) + x^T(t) W_i x(t), \quad (22) \end{aligned}$$

in which

$$\begin{aligned} W_i &= \Delta L_{i,1} - \Delta L_{i,2} - \Delta L_{i,3}, \\ \Delta L_{i,1} &= P_i \hat{C}_i \Delta A_i + \Delta A_i^T P_i, \\ \Delta L_{i,2} &= P_i N_i C_i \Delta A_i + \Delta A_i^T C_i^T N_i^T P_i, \\ \Delta L_{i,3} &= P_i N_i K_i + K_i^T N_i^T P_i. \quad (23) \end{aligned}$$

By substituting (11) and (13) into (23), we obtain

$$\begin{aligned} \Delta L_{i,2} &= \Delta L_{i,21} + \Delta L_{i,22} + \Delta L_{i,23}, \\ \Delta L_{i,3} &= \Delta L_{i,31} + \Delta L_{i,32} + \Delta L_{i,33}, \quad (24) \end{aligned}$$

where

$$\begin{aligned} \Delta L_{i,21} &= P_i \Delta B_i (C_i B_i)^{-1} C_i \Delta A_i + [P_i \Delta B_i (C_i B_i)^{-1} C_i \Delta A_i]^T, \\ \Delta L_{i,22} &= P_i B_i M_i (C_i B_i)^{-1} C_i \Delta A_i + [P_i B_i M_i (C_i B_i)^{-1} C_i \Delta A_i]^T, \\ \Delta L_{i,23} &= P_i \Delta B_i M_i (C_i B_i)^{-1} C_i \Delta A_i \\ &\quad + [P_i \Delta B_i M_i (C_i B_i)^{-1} C_i \Delta A_i]^T, \\ \Delta L_{i,31} &= P_i \Delta B_i (C_i B_i)^{-1} K_i + [P_i \Delta B_i (C_i B_i)^{-1} K_i]^T, \\ \Delta L_{i,32} &= P_i B_i M_i (C_i B_i)^{-1} K_i + [P_i B_i M_i (C_i B_i)^{-1} K_i]^T, \\ \Delta L_{i,33} &= P_i \Delta B_i M_i (C_i B_i)^{-1} K_i + [P_i \Delta B_i M_i (C_i B_i)^{-1} K_i]^T. \end{aligned}$$

Then, according to Assumption 2, Lemma 1 and (12), for arbitrary positive numbers  $\varepsilon_{i,1}, \varepsilon_{i,21}, \varepsilon_{i,22}, \varepsilon_{i,23}, \varepsilon_{i,31}, \varepsilon_{i,32}$  and  $\varepsilon_{i,33}$ , the following inequalities hold true:

$$\begin{aligned} \Delta L_{i,1} &\leq \varepsilon_{i,1}^{-1} P_i \hat{C}_i H_{a,i} H_{a,i}^T \hat{C}_i^T P_i + \varepsilon_{i,1} E_{a,i}^T E_{a,i}, \\ \Delta L_{i,21} &\leq \varepsilon_{i,21}^{-1} \delta_{i,1} P_i H_{b,i} H_{b,i}^T P_i + \varepsilon_{i,21} E_{a,i}^T E_{a,i}, \\ \Delta L_{i,22} &\leq \frac{\varepsilon_{i,22}^{-1} \delta_{i,1} \delta_{i,2}}{(1 - \gamma_i)^2} P_i B_i (C_i B_i)^{-1} (C_i B_i)^{-T} B_i^T P_i \\ &\quad + \varepsilon_{i,22} E_{a,i}^T E_{a,i}, \\ \Delta L_{i,23} &\leq \frac{\varepsilon_{i,23}^{-1} \delta_{i,1} \delta_{i,2} \delta_{i,3}}{(1 - \gamma_i)^2} P_i H_{b,i} H_{b,i}^T P_i + \varepsilon_{i,23} E_{a,i}^T E_{a,i}, \\ \Delta L_{i,31} &\leq \varepsilon_{i,31}^{-1} P_i H_{b,i} H_{b,i}^T P_i + \varepsilon_{i,31} \bar{E}_{b,i}^T \bar{E}_{b,i}, \\ \Delta L_{i,32} &\leq \frac{\varepsilon_{i,32}^{-1} \delta_{i,2}}{(1 - \gamma_i)^2} P_i B_i (C_i B_i)^{-1} (C_i B_i)^{-T} B_i^T P_i \\ &\quad + \varepsilon_{i,32} \bar{E}_{b,i}^T \bar{E}_{b,i}, \\ \Delta L_{i,33} &\leq \frac{\varepsilon_{i,33}^{-1} \delta_{i,2} \delta_{i,3}}{(1 - \gamma_i)^2} P_i H_{b,i} H_{b,i}^T P_i + \varepsilon_{i,33} \bar{E}_{b,i}^T \bar{E}_{b,i}. \end{aligned}$$

The values of  $\varepsilon_{i,1}, \varepsilon_{i,21}, \varepsilon_{i,22}, \varepsilon_{i,23}, \varepsilon_{i,31}, \varepsilon_{i,32}$  and  $\varepsilon_{i,33}$  are all set to  $\varepsilon_i$ , and the following relation holds true by (23) and (24):

$$W_i \leq \varepsilon_i^{-1} P_i \Omega_i P_i + 4\varepsilon_i E_{a,i}^T E_{a,i} + 3\varepsilon_i \bar{E}_{b,i}^T \bar{E}_{b,i}, \quad (25)$$

where

$$\Omega_i = \hat{C}_i H_{a,i} H_{a,i}^T \hat{C}_i^T + \tau_{i,1}^2 H_{u,i} H_{u,i}^T + \tau_{i,2}^2 H_{b,i} H_{b,i}^T.$$

As described in (22) and (25), according to the Schur complement lemma, if LMIs (17) can be satisfied,  $\dot{V}_i(t) < 0$ ; i.e., each subsystem in the sliding mode as described by (14) is of robust stability and thereby the robust stable matrix set is constructed. ■

*Remark 3:* By contrast with the RISM design in [25], the presented SRISM (7) in this paper comprises of the switched parameters  $C_i$  and  $K_i$ . Therefore, the LMIs conditions in Theorem 1 are easier to be resolved.

### C. SRISM SLIDING SURFACE AND ITS STABILITY

The sliding mode (7) of every subsystem (2) has been designed and the corresponding sliding mode dynamic (15) is obtained. Moreover, the subsystem matrices  $\hat{A}_i$  comprise a robust stable matrix set  $\hat{\mathbb{A}}$  if the parameter matrix  $K_i$  satisfies Theorem 1. This means that every sliding mode dynamic (15) of every subsystem is robustly stable with respect to uncertainty and disturbance

However, the whole switched system (15) under the switching signal  $\sigma(t)$  (the switching sequence  $Q$ ) is not ensured to be robustly stable, even though every subsystem matrix  $\hat{A}_i$  displays robust stability.

Assuming that the system state  $x$  runs onto the corresponding RISM surface and remains there when the switching  $\sigma(t) = i$  occurs at the time  $t_k$ . This property can be easily ensured because  $S_i(x(t_k), t_k) = 0$  by (7). Consequently, it is important to keep state  $x$  on the RISM surface at all times,

which is carried out by the sliding mode controller. If we consider that this is achieved, the sliding surface with multiple sliding modes for the SS (1) is obtained as (6). This method can also be called the switched RISM (SRISM) because its component  $S_i(x, t) = 0$  is the RISM. Now, we can state that the system state  $x$  is on the sliding surface or the SRISM  $S(x, t)$ . Namely, the switched system (2) is under its *sliding mode*.

When the system state  $x$  is running under the *sliding mode* of the switched system (2), its stability depends on the dynamic (15). There are two typical approaches for guaranteeing the stability of SRISM based on the robust stable matrix set  $\hat{\mathbb{A}}$  for which every matrix element  $\hat{A}_i$  satisfies Theorem 1.

### 1) COMMON LYAPUNOV FUNCTION

**Theorem 2:** The switched system dynamic (15) under the sliding mode  $S(x, t)$  is robustly stable with respect to the uncertainty and disturbance with arbitrary time-dependent switching signal, if there exist a symmetric positive definite matrix  $P$  and the corresponding positive scalar  $\varepsilon_i$  satisfy LMIs (17). Namely, the LMIs

$$\begin{bmatrix} \Theta_i & P\hat{C}_iH_{a,i} & \tau_{i,1}PH_{u,i} & \tau_{i,2}PH_{b,i} \\ * & -\varepsilon_iI_{r_a \times r_a} & 0 & 0 \\ * & * & -\varepsilon_iI_{m \times m} & 0 \\ * & * & * & -\varepsilon_iI_{r_b \times r_b} \end{bmatrix} < 0, \quad (26)$$

hold true with

$$\Theta_i = P\hat{A}_i + \hat{A}_i^T P + 4\varepsilon_i E_{a,i}^T E_{a,i} + 3\varepsilon_i \bar{E}_{b,i}^T \bar{E}_{b,i}. \quad (27)$$

with  $\tau_{i,1}, \tau_{i,2}$  following (19), (20).

**Remark 4:** Matrix  $P$  clearly generates a common Lyapunov function  $V(t) = x^T(t)Px(t)$  for which time derivative  $\dot{V}(t) < 0$ . Then, the conclusion of Theorem 2 is reached.

### 2) STABILIZATION WITH THE SWITCHING SIGNAL DESIGN

If the switching signal  $\sigma(t)$  can be designed arbitrarily, the switched system (15) under the sliding mode  $S(x, t)$  will be stabilized by the switching signal.

Define the switching district  $\mathcal{D}_i, \forall i, j \in \mathbb{N}$  of the state  $x(t) \in \mathbb{R}^n$  as

$$\mathcal{D}_i = \left\{ x(t) \mid x^T(t)(P_i - P_j)x(t) \leq 0, j \neq i \right\}, \quad (28)$$

we obtain the following result [33] based on multiple Lyapunov functions method.

**Theorem 3:** If the parameter  $K_i$  in the sliding mode (7) and the positive definite symmetric matrix  $P_i$  satisfy Theorem 1, such that  $\hat{\mathbb{A}} = \{\hat{A}_1, \hat{A}_2, \dots, \hat{A}_N\}$  forms the set of robust stable matrices, then the sliding mode (15),(16) is robustly stable under the control of the switching sequence of the following switching rules

$$\sigma(t_0) = \arg \min_{i \in \mathbb{N}} \left\{ x^T(t_0) P_i x(t_0), x(t_0) \in \mathbb{R}^n \right\}, \quad (29)$$

$$\sigma(t_k) = \begin{cases} i, & \text{if } x(t_k) \in \mathcal{D}_i \text{ and } \sigma(t_{k-1}) = i; \\ \arg \min_{i \in \mathbb{N}} \{ x^T(t)(P_i - P_j)x(t) \}, & \\ i, & \text{if } x(t_k) \in \mathcal{D}_i \text{ and } \sigma(t_{k-1}) = j, j \neq i. \end{cases} \quad (30)$$

## IV. SMC CONTROLLER

### A. SLIDING MODE CONTROL DESIGN

The equivalent control described in (10) is not feasible since it includes many uncertainties and disturbance. Therefore, a sliding mode controller is designed according to:

$$u(t) = -(C_i B_i)^{-1} [K_i x(t) + \kappa_i S_i(t) + (\rho_i + \eta_i \|x(t)\|) \text{sgn} S_i(t)], \quad (31)$$

for which the parameters are designed as

$$\rho_i \geq (1 - \gamma_i)^{-1} [\mu_i + d_i (\|C_i B_i\| + \|C_i H_{b,i}\| \|E_{b,i}\|)], \quad (32)$$

$$\eta_i \geq (1 - \gamma_i)^{-1} [\|C_i H_{a,i}\| \|E_{a,i}\| + \|C_i H_{b,i}\| \|E_{b,i}\| (C_i B_i)^{-1} K_i]. \quad (33)$$

Here,  $\kappa_i, \mu_i > 0$  are optional positive scalars.

### B. REACHABILITY OF THE DESIGNED SLIDING MODES

**Theorem 4:** For the switched system (2) and its corresponding robust integral sliding mode (7), the sliding mode controller (31), (32) and (33) makes the system's state trajectory reach the sliding surface ( $S_i(x, t) = 0$ ) from the initial time  $t_k$  and remaining on the sliding surface.

**Proof:** The following Lyapunov function is selected:

$$V(t) = \sum_{i=1}^N \lambda_i S_i^T(x, t) S_i(x, t).$$

The time derivative of the function then can be calculated according to the sliding mode function (7):

$$\dot{V}(t) = \sum_{i=1}^N \lambda_i S_i^T(x, t) [(C_i \Delta A_i + K_i)x(t) + (C_i B_i + C_i \Delta B_i)(u(t) + \omega_i(t))].$$

Substituting the controller (31) into the above time derivative expression, we obtain the following expression:

$$\begin{aligned} \dot{V}(t) = & \sum_{i=1}^N \lambda_i S_i^T(x, t) [C_i \Delta A_i x(t) - C_i \Delta B_i (C_i B_i)^{-1} K_i x(t) \\ & + (C_i B_i + C_i \Delta B_i) \omega_i(t) - (\rho_i + \eta_i \|x(t)\|) \text{sgn} S_i(x, t) \\ & - \kappa_i S_i(x, t) - \kappa_i C_i \Delta B_i (C_i B_i)^{-1} S_i(x, t) \\ & - C_i \Delta B_i (C_i B_i)^{-1} (\rho_i + \eta_i \|x(t)\|) \text{sgn} S_i(x, t)]. \end{aligned} \quad (34)$$

According to the design principle (8) of the matrix  $C_i$ , the following expression is true:

$$C_i \Delta B_i (C_i B_i)^{-1} \leq \gamma_i I. \quad (35)$$



According to (35), Assumption 2 and Assumption 3, the following inequality based on (34) can be obtained:

$$\begin{aligned} \dot{V}(t) \leq & \sum_{i=1}^N \lambda_i [(\|C_i H_{a,i}\| \|E_{a,i}\| \\ & + \|C_i H_{b,i}\| \|E_{b,i}(C_i B_i)^{-1} K_i\|) \|x(t)\| \|S_i(x, t)\| \\ & + d_i(\|C_i B_i\| + \|C_i H_{b,i}\| \|E_{b,i}\|) \|S_i(x, t)\| \\ & - (1 - \gamma_i)(\rho_i + \eta_i \|x(t)\|) \|S_i(x, t)\| \\ & - (1 - \gamma_i) \kappa_i \|S_i(x, t)\|^2]. \end{aligned} \quad (36)$$

According to the parameter design principles (32) and (33) of the controller (31), the inequality (36) can be rewritten as:

$$\dot{V}(t) \leq - \sum_{i=1}^N \lambda_i [\mu_i \|S_i(x, t)\| + (1 - \gamma_i) \kappa_i \|S_i(x, t)\|^2].$$

This means that the RISM of the system (2) is asymptotically stable and the system state will keep moving on the sliding surface  $S_i(x, t) = 0$  from the switching initial time  $t_k$  because of  $S_i(x(t_k), t_k) = 0$ . That is, the RISM hyperplane (7) is reached from the initial time  $t_k$  only if the initial state value  $x(t_k)$  is known. ■

*Remark 5:* Theorem 4 shows that the sliding mode controller (31) makes every RISM of every subsystem reached from the initial time  $t_k$ , when the switching occurs. Therefore, all of the  $S_i(x, t) = 0$  following the switching sequence  $Q$  will comprise the sliding surface with multiple sliding modes defined in Definition 1.

## V. ILLUSTRATIVE EXAMPLES

### A. NUMERICAL SIMULATION

A switched system (1) consisting of three subsystems was simulated when the system state is measurable. Namely  $\mathbb{N} \doteq \{1, 2, 3\}$ . The parameters of the system are listed below.

$$\begin{aligned} A_1 &= \begin{bmatrix} -1 & 1 \\ 2 & -4 \end{bmatrix}, A_2 = \begin{bmatrix} 1 & 3 \\ 10 & 0 \end{bmatrix}, A_3 = \begin{bmatrix} 0 & 0 \\ 3 & 7 \end{bmatrix}, \\ B_1 &= \begin{bmatrix} 0 \\ 1 \end{bmatrix}, B_2 = \begin{bmatrix} 1 \\ 1 \end{bmatrix}, B_3 = \begin{bmatrix} 1 \\ 1 \end{bmatrix}, \\ \Delta A_1 &= \begin{bmatrix} 0.38 \sin 4\pi t & 0 \\ 0 & 0.4e^{-t} \end{bmatrix}, \\ \Delta A_2 &= \begin{bmatrix} 0.65 \cos 7\pi t & 0.2 \cos 7\pi t \\ 0 & 0.56e^{-2.2t} \end{bmatrix}, \\ \Delta A_3 &= \begin{bmatrix} 0 & 0 \\ 0.34 \sin 2\pi t & 0.3e^{-t^2} \end{bmatrix}, \\ \Delta B_1 &= [0 \quad 0.15e^{-3t}]^T, \quad \Delta B_2 = [0.36 \cos 4\pi t \quad 0]^T, \\ \Delta B_3 &= [0 \quad 0.1e^{-1.8t} + 0.3 \sin 8\pi t]^T. \end{aligned}$$

It can be proved that  $\forall i \in \mathbb{N}$ ,  $(A_i, B_i)$  can be stabilizable. According to Assumption 2, the uncertainties are decomposed as the following matrices.

Subsystem 1:

$$\begin{aligned} H_{a,1} &= \begin{bmatrix} 1 & 0 \\ 0 & 1 \end{bmatrix}, F_{a,1} = \begin{bmatrix} \sin 4\pi t & 0 \\ 0 & e^{-t} \end{bmatrix}, F_{b,1} = e^{-3t}, \\ E_{a,1} &= \begin{bmatrix} 0.38 & 0 \\ 0 & 0.4 \end{bmatrix}, H_{b,1} = \begin{bmatrix} 0 \\ 1.5 \end{bmatrix}, E_{b,1} = 0.1. \end{aligned}$$

Subsystem 2:

$$\begin{aligned} H_{a,2} &= \begin{bmatrix} 1 & 0 \\ 0 & 1 \end{bmatrix}, F_{a,2} = \begin{bmatrix} \cos 7\pi t & 0 \\ 0 & e^{-2.2t} \end{bmatrix}, E_{b,2} = 0.36, \\ E_{a,2} &= \begin{bmatrix} 0.65 & 0.2 \\ 0 & 0.56 \end{bmatrix}, H_{b,2} = \begin{bmatrix} 1 \\ 0 \end{bmatrix}, F_{b,2} = \cos 4\pi t, \end{aligned}$$

Subsystem 3:

$$\begin{aligned} H_{a,3} &= \begin{bmatrix} 0 & 0 \\ 0.2 & 0.2 \end{bmatrix}, F_{a,3} = \begin{bmatrix} \sin 2\pi t & 0 \\ 0 & e^{-t^2} \end{bmatrix}, \\ H_{b,3} &= \begin{bmatrix} 0 & 0 \\ 0.5 & 0.5 \end{bmatrix}, \\ F_{b,3} &= \begin{bmatrix} e^{-1.8t} & 0 \\ 0 & \sin 8\pi t \end{bmatrix}, E_{a,3} = \begin{bmatrix} 1.7 & 0 \\ 0 & 1.5 \end{bmatrix}, E_{b,3} = \begin{bmatrix} 0.2 \\ 0.6 \end{bmatrix}. \end{aligned}$$

According to the parameter design conditions (8), the parameters  $C_1 = [2, 1]$ ,  $C_2 = [1, 1]$ ,  $C_3 = [1, 0]$  are selected. It can be verified that  $\forall i \in \mathbb{N}$ ,  $C_i B_i$  is non-singular. Moreover, the parameter design conditions (8) are verified.

Subsystem 1:  $C_1 \Delta B_1 = 0.15e^{-3t}$ , select  $\gamma_1 = 0.15$ .

Subsystem 2:  $C_2 \Delta B_2 = 0.36 \cos 4\pi t$ , select  $\gamma_2 = 0.18$ .

Subsystem 3:  $C_3 \Delta B_3 = 0$ , select  $\gamma_3 = 0.1$ .

To select the matrices  $K_1 = [23, 7]$ ,  $K_2 = [60, 30]$ ,  $K_3 = [-18, 200]$ , then  $\hat{A}_i, H_{u,i}, \hat{C}_i, \hat{E}_{b,i}, \tau_{i,1}, \tau_{i,2}$  are determined based on the above-described parameters and (18),(19).

After the above-described calculations, it can be verified whether  $C_i$  and  $K_i$  can make  $\hat{A}_i, i \in \mathbb{N}$  be a robust stable matrix set based on Theorem 1. We can directly solve (17). Using the LMI toolbox in Matlab, the three LMIs of three subsystems were solved. The matrices  $P_1, P_2, P_3$  are found to be:

$$\begin{aligned} P_1 &= \begin{bmatrix} 2.916 & 0.407 \\ 0.407 & 0.136 \end{bmatrix}, P_2 = \begin{bmatrix} 1.457 & 0.418 \\ 0.418 & 0.334 \end{bmatrix}, \\ P_3 &= \begin{bmatrix} 0.273 & -0.902 \\ -0.902 & 8.331 \end{bmatrix}. \end{aligned}$$

Thus, the SRISMs (7) are obtained.

We set the system state initial value as  $x(t_0) = [0.4, 0.8]^T$ . The sliding mode controller under the designed switching rules (29),(30) can be written as (31) by Theorem 4, for which  $\rho_i = 20$  and  $\eta_i = 10$  are set according to (32) and (33). By substituting  $C_i, K_i, A_i$  and  $B_i$  into (31), the practical switched controller can be obtained.

Figs. 1-3 display the simulation results of the switched system from which we can observe that under the existence of uncertain parameters and external disturbances, the system state remains on the sliding surface with the designed switching rule from the initial time onward.

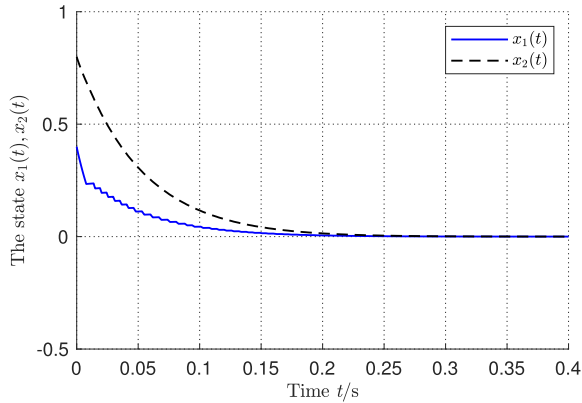


FIGURE 1. State trajectories of the switched system.

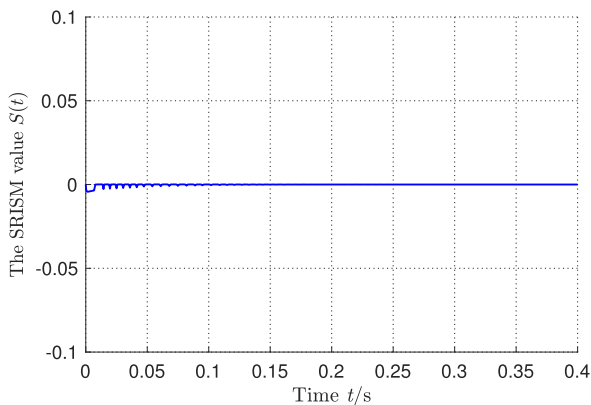


FIGURE 2. SRISM value  $S(x, t)$  of the switched system.

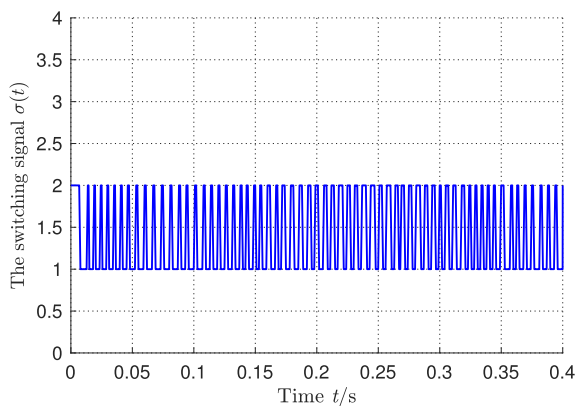


FIGURE 3. Switching signal  $\sigma(t)$ .

*Remark 6:* For the numerical example in this subsection, the CRISM as the design method in [25] was not found. The different matrices  $\hat{A}_i$  are obtained because of the switched parameters  $C_i, K_i$ . The LMIs conditions in the result of Theorem 4 in [25] were tried to be resolved, but there were no solutions.

### B. APPLICATION SIMULATION

A classical single inverted pendulum (SIP) system is considered, for which the mathematical model is given by

$$\ddot{\theta}(t) = \frac{(M+m)g\sin\theta(t) - ml\dot{\theta}^2(t)\sin\theta(t)\cos\theta(t) - F\cos\theta(t)}{l\left[\frac{4}{3}(M+m) - m\cos^2\theta(t)\right]}, \quad (37)$$

where  $\theta(t)$  denotes the angle of the pendulum,  $F$  represents the control force of the cart that moves in a straight line,  $M = 1.1\text{kg}$  is the mass of the cart,  $m = 0.12\text{kg}$  is the mass of the pendulum,  $l = 0.25\text{m}$  is the distance to the mass center of the pendulum, and  $g = 9.8\text{m} \cdot \text{s}^{-2}$  is the acceleration due to gravity.

It is well-known that the SIP system has two typical equilibrium states. The first is the upper position where the pendulum can be held inversely, and the other one is the lower position where the pendulum swings down to the steady point naturally. Therefore, the SIP system at the two positions can be modeled as two linear time-invariant (LTI) systems, respectively. To carry out the calculations,  $x_1(t) = \theta(t)$ ,  $x_2(t) = \dot{\theta}(t)$  are set as the state variables that comprise the state vector  $x(t) = [x_1(t), x_2(t)]^T$ , and the origin point  $x_1(t) = 0$  is responding to the upper position point.

Consequently, the nonlinear dynamic (37) is linearized at the two points:  $x_1(t) \approx 0$  and  $x_1(t) \approx \pi$ . The following two LTI systems are obtained

$$\begin{aligned} \dot{x}(t) &= A_{\sigma(t)}x(t) + B_{\sigma(t)}u, \quad \sigma(t) = 1, 2, \\ A_1 &= \begin{bmatrix} 0 & 1 \\ -31.7416 & 0 \end{bmatrix}, \quad A_2 = \begin{bmatrix} 0 & 1 \\ 31.7416 & 0 \end{bmatrix}, \\ B_1 &= \begin{bmatrix} 0 \\ 2.6549 \end{bmatrix}, \quad B_2 = \begin{bmatrix} 0 \\ -2.6549 \end{bmatrix}, \end{aligned} \quad (38)$$

where the system matrices  $A_1, B_1$  represent the lower position and the system matrices  $A_2, B_2$  represent the upper position. To apply and verify the design method presented in this paper, we assume that

$$\begin{aligned} \Delta A_1 &= \begin{bmatrix} 0 & 0 \\ 8\sin 4t & \cos 7t \end{bmatrix}, \quad \Delta A_2 = \begin{bmatrix} 0 & 0 \\ 7\cos 5t & 2\sin 3t \end{bmatrix}, \\ \Delta B_1 &= \begin{bmatrix} 0 \\ 0.3\sin t \end{bmatrix}, \quad \Delta B_2 = \begin{bmatrix} 0 \\ 0.12\cos t \end{bmatrix} \end{aligned}$$

denote the uncertainties of  $A_1, A_2, B_1, B_2$ , respectively. They all can be decomposed by Assumption 2. Then, we selected  $C_1 = [1, 1]$ ,  $C_2 = [1, -0.5]$  and  $K_1 = [24, 12]$ ,  $K_2 = [-25, -4]$  to obtain the appropriate roots of  $\hat{A}_1$  and  $\hat{A}_2$ . According to Theorem 1, we obtained the solutions of  $P_1, P_2$  for LMIs (17) as:

$$P_1 = \begin{bmatrix} 1.01 & 0.0076 \\ 0.0076 & 0.0172 \end{bmatrix}, \quad P_2 = \begin{bmatrix} 13.61 & 1.36 \\ 1.36 & 0.4236 \end{bmatrix}.$$

As a result, the two RISMs are obtained by (7), and the controller is designed by (31) after selecting the parameters  $\kappa_1 = 200$ ,  $\kappa_2 = 50$ ,  $\rho_1 = 5$ ,  $\rho_2 = 0.5$ ,  $\eta_1 = 20$ ,  $\eta_2 = 10$ . To ensure the stability of the two subsystems (38) while switching, we found their common Lyapunov function

matrix  $P = \begin{bmatrix} 0.628 & 0.0398 \\ 0.0398 & 0.015 \end{bmatrix}$  by Theorem 2. This means that the switched system (38) can theoretically be stabilized by the SMC controller under any switching rule.

However, the two subsystems in (38) only represent the models near the two equilibrium states. The real control plant is the nonlinear dynamic (37). Now, we consider the swing-up control problem for the SIP system. The initial state value is set as  $x(t) = [\pi, 0]^T$ . The key solution is for the switching rule between the lower sub-controller  $u_1$  and the upper sub-controller  $u_2$ . It is clear that the lower sub-controller  $u_1$  must be operated when the angle  $x_1(t)$  approaches  $\pi$  and the upper sub-controller  $u_2$  must be operated while  $x_1(t)$  approaches 0. The difficulty lies in using the controller when the angle  $x_1(t)$  approaches  $\pi/2$  or  $3\pi/2(-\pi/2)$ . Therefore, we designed the following switching rules  $\sigma_j(t)$ . ( $\sigma(t) = 3$  means none of the two sub-controllers be used, i.e.,  $u_3(t) = 0$ )

- 1)  $\|\theta(t)\| \geq \frac{2\pi}{3}, \sigma_1(t) = 1; \|\theta(t)\| < \frac{2\pi}{3}, \sigma_1(t) = 2.$
- 2)  $\|\theta(t)\| \geq \frac{2\pi}{3}, \sigma_2(t) = 1; \|\theta(t)\| \leq \frac{\pi}{4}, \sigma_2(t) = 2;$  otherwise  $\sigma_2(t) = 3;$
- 3)  $\|\theta(t)\| \geq \frac{2\pi}{3}, \sigma_3(t) = 1; \|\theta(t)\| \leq \frac{\pi}{5}, \sigma_3(t) = 2;$  otherwise  $\sigma_3(t) = 3;$
- 4)  $\|\theta(t)\| \geq \frac{2\pi}{3}, \sigma_4(t) = 1; \|\theta(t)\| \leq \frac{\pi}{6}, \sigma_4(t) = 2;$  otherwise  $\sigma_4(t) = 3;$
- 5)  $\|\theta(t)\| \geq \frac{2\pi}{3}, \sigma_5(t) = 1; \|\theta(t)\| \leq \frac{\pi}{10}, \sigma_5(t) = 2;$  otherwise  $\sigma_5(t) = 3.$

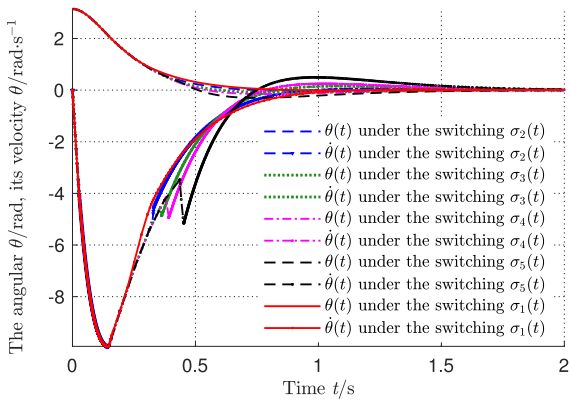


FIGURE 4. Angle and angular velocity trajectories of the SIP system.

All of the switching rules  $\sigma_j(t), j = 1, 2, \dots, 5$  were operated in the simulation of the SIP system and the corresponding simulation results are shown in Fig. 4-Fig. 7. WE Note that the nonlinear dynamic (37) was used as the controlled plant and the two sub-controllers were designed as mentioned above in this subsection.

Fig. 4 shows that the pendulum can be swung up by all of the five switching rules and the transient performance characteristics of the angle  $\theta(t)$  are nearly the same. However, the negative angular velocity  $\dot{\theta}(t)$  changes its rapid variation trend and has jump by the switching signal  $\sigma(t)$ .

The reasons of the jump of  $\dot{\theta}(t)$  in Fig. 4 were essentially related to the switching strategy of  $\sigma(t)$ . By the switching rule  $\sigma_1(t)$ , the switching signal has two values  $\sigma_1(t) = 1$

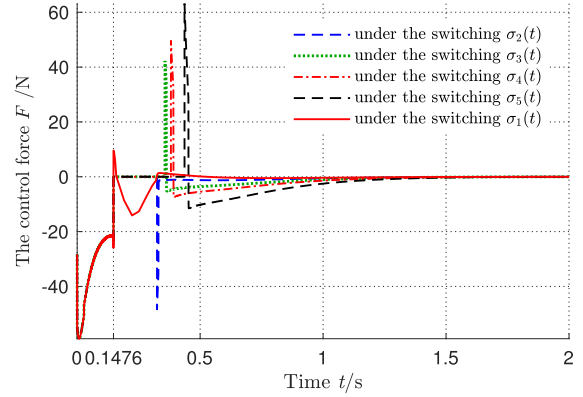


FIGURE 5. Control force curves of the SIP system.

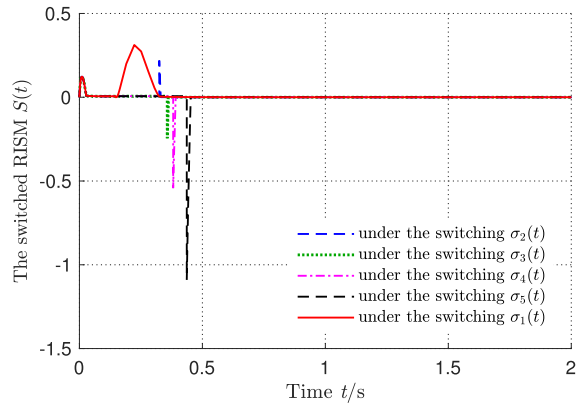


FIGURE 6. Switched RISM signals of the SIP system.

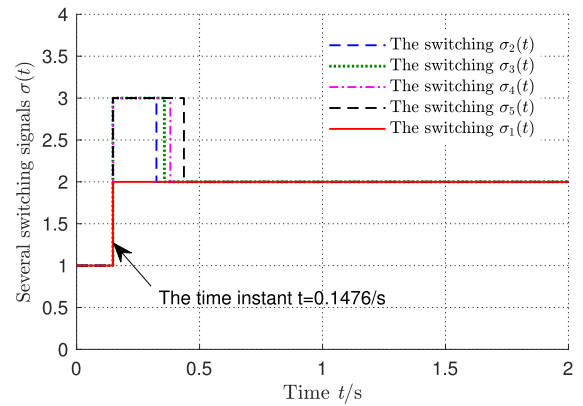


FIGURE 7. Switching signals adopted for the SIP swing-up.

and  $\sigma_1(t) = 2$ , that leads to the two control force signals  $u_1(t)$  and  $u_2(t)$  which were all stabilizing the state variables. Therefore,  $\dot{\theta}(t)$  under the switching  $\sigma_1(t)$  has no jump. By the switching rule  $\sigma_j(t), \forall j = 2, 3, 4, 5$ , the switching signal has three values  $\sigma_j(t) = 1, \sigma_j(t) = 2$  and  $\sigma_j(t) = 3$ , that leads to the two control force signals  $u_1(t), u_2(t)$  and the zero control force signal  $u_3(t) = 0$ . Therefore,  $\dot{\theta}(t)$  has the jump due to the zero control force. When the control force  $u_3(t) = 0$ ,  $\dot{\theta}(t)$  would jump to the inverse running direction after the inertia force ends and before the new force  $u_2(t)$  starts. The jump will have the elongation while  $u_3(t) = 0$  lasts the longer time.



Fig. 5 clearly demonstrates that the control force switched while the switching signal changes. For example, the control force  $F$  switched to another signal at  $t = 0.1476$  s because at this moment,  $\theta(t) < \frac{2\pi}{3}$  under the switching rule  $\sigma_1(t)$ . We decreased  $\eta_2 = 1$  at this rule to reduce the control force jump. The sliding surface consisting of the two SRISMs varied at the switching time, as shown in Fig. 6. The sliding surface value showed clear continuous jumping at each switching time. This is because the dynamic of the control plant is close to the complicated nonlinear dynamic (37), but is not similar to the switched dynamic in (1). Nevertheless, the sliding surface value was quickly driven to values close to zero by the control force. Fig. 7 shows the switching signals for all of the switching rules.

An examination of Fig. 4-Fig. 7 reveals an interesting phenomenon that the impact of the controller switching may be slightly stronger for the later switching to the sub-controller of the upper position (Switching to the upper position equilibrium state at smaller  $\theta(t)$ ). Among these five switching rules, the best swing-up performance is obtained under the switching rule  $\sigma_1(t)$  event though the sub-controller  $u_2$  has been operated early following the lower position without waiting. It is possible that assumptions such a no friction, no measurement delays are required. To summarize, the simulation results validated the validity of the swing-up control design by the SMC method based on the sliding surface with multiple sliding modes (or the switched integral sliding mode).

## VI. CONCLUSION

A new switched robust integral sliding mode (SRISM) for uncertain switched systems with unmatched uncertainties was studied. The proposed sliding surface with multiple sliding modes is also switched by the switching rule forming SRISM and has the ability to reject the unmatched uncertainties. The system state does not need to jump between the switching of the sliding modes because the integral sliding modes will be reached starting from the switching time. The stability of the switched system (SS) under this proposed SRISM is ensured by two typical approaches. The first is the common Lyapunov function method, and the second is the stabilization via the switching rule. Numerical and application simulation results were used to illustrate the theoretical results. In the simulation of the application of this method of a single pendulum inverted system, the pendulum can be swung up by the designed switching rules and the SMC sub-controllers based on the SRISM. These simulations validated the effectiveness of the proposed method.

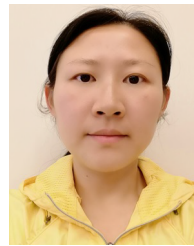
## ACKNOWLEDGMENT

The author would like to thank the Editors and the Reviewers for their contributions.

## REFERENCES

- [1] H. Lin and P. J. Antsaklis, "Stability and stabilizability of switched linear systems: A survey of recent results," *IEEE Trans. Autom. Control*, vol. 54, no. 2, pp. 308–322, Feb. 2009.
- [2] L. Wu, P. Shi, and X. Su, *Sliding Mode Control of Uncertain Parameter-Switching Hybrid Systems*. Hoboken, NJ, USA: Wiley, 2014.
- [3] J. Wang, S. Huo, J. Xia, J. H. Park, X. Huang, and H. Shen, "Generalised dissipative asynchronous output feedback control for Markov jump repeated scalar non-linear systems with time-varying delay," *IET Control Theory Appl.*, vol. 13, no. 13, pp. 2114–2121, Sep. 2019.
- [4] T. Ru, J. Xia, X. Huang, X. Chen, and J. Wang, "Reachable set estimation of delayed fuzzy inertial neural networks with Markov jumping parameters," *J. Franklin Inst.*, vol. 357, no. 11, pp. 6882–6898, Jul. 2020.
- [5] M. Xing, J. Xia, X. Huang, and H. Shen, "On dissipativity-based filtering for discrete-time switched singular systems with sensor failures: A persistent dwell-time scheme," *IET Control Theory Appl.*, vol. 13, no. 12, pp. 1814–1822, Aug. 2019.
- [6] L. Wu and J. Lam, "Sliding mode control of switched hybrid systems with time-varying delay," *Int. J. Adapt. Control Signal Process.*, vol. 22, no. 10, pp. 909–931, Dec. 2008.
- [7] L. Wu, D. W. C. Ho, and C. W. Li, "Sliding mode control of switched hybrid systems with stochastic perturbation," *Syst. Control Lett.*, vol. 60, no. 8, pp. 531–539, Aug. 2011.
- [8] T. R. Oliveira, A. J. Peixoto, and L. Hsu, "Sliding mode control of uncertain multivariable nonlinear systems with unknown control direction via switching and monitoring function," *IEEE Trans. Autom. Control*, vol. 55, no. 4, pp. 1028–1034, Apr. 2010.
- [9] L. Wu, X. Su, and P. Shi, "Sliding mode control with bounded gain performance for Markovian jump singular time-delay systems," *Automatica*, vol. 48, no. 8, pp. 1929–1933, Aug. 2012.
- [10] M. Tanelli and A. Ferrara, "Enhancing robustness and performance via switched second order sliding mode control," *IEEE Trans. Autom. Control*, vol. 58, no. 4, pp. 962–974, Apr. 2013.
- [11] Y. Wang, V. Gupta, and P. J. Antsaklis, "On passivity of a class of discrete-time switched nonlinear systems," *IEEE Trans. Autom. Control*, vol. 59, no. 3, pp. 692–702, Mar. 2014.
- [12] Y. Liu, T. Jia, Y. Niu, and Y. Zou, "Design of sliding mode control for a class of uncertain switched systems," *Int. J. Syst. Sci.*, vol. 46, no. 6, pp. 993–1002, Apr. 2015.
- [13] Y. Liu, H. R. Karimi, Y. Zou, and Y. Niu, "Adaptive sliding mode reliable control for switched systems with actuator degradation," *IET Control Theory Appl.*, vol. 9, no. 8, pp. 1197–1204, May 2015.
- [14] A. Pisano, M. Tanelli, and A. Ferrara, "Switched/time-based adaptation for second-order sliding mode control," *Automatica*, vol. 64, pp. 126–132, Feb. 2016.
- [15] X. Su, X. Liu, P. Shi, and R. Yang, "Sliding mode control of discrete-time switched systems with repeated scalar nonlinearities," *IEEE Trans. Autom. Control*, vol. 62, no. 9, pp. 4604–4610, Sep. 2017.
- [16] Y. Qi and J. Hu, "Observer-based bumpless switching control for switched linear systems with sensor faults," *Trans. Inst. Meas. Control*, vol. 40, no. 5, pp. 1490–1498, Mar. 2018.
- [17] H. Zhao, Y. Niu, and J. Song, "Finite-time output feedback control of uncertain switched systems via sliding mode design," *Int. J. Syst. Sci.*, vol. 49, no. 5, pp. 984–996, Apr. 2018.
- [18] J. Wang, C. Yang, H. Shen, J. Cao, and L. Rutkowski, "Sliding-mode control for slow-sampling singularly perturbed systems subject to Markov jump parameters," *IEEE Trans. Syst., Man, Cybern. Syst.*, early access, Mar. 24, 2020, doi: 10.1109/TSMC.2020.2979860.
- [19] V. Utkin and J. Shi, "Integral sliding mode in systems operating under uncertainty conditions," in *Proc. 35th IEEE Conf. Decis. Control*, Dec. 2002, pp. 4591–4596.
- [20] W.-J. Cao and J.-X. Xu, "Nonlinear integral-type sliding surface for both matched and unmatched uncertain systems," *IEEE Trans. Autom. Control*, vol. 49, no. 8, pp. 1355–1360, Aug. 2004.
- [21] J. Lian, J. Zhao, and G. M. Dimirovski, "Integral sliding mode control for a class of uncertain switched nonlinear systems," *Eur. J. Control*, vol. 16, no. 1, pp. 16–22, Jan. 2010.
- [22] J. Lian and J. Zhao, "Robust  $h_\infty$  integral sliding mode control for a class of uncertain switched nonlinear systems," *J. Control Theory Appl.*, vol. 8, no. 4, pp. 521–526, 2010.
- [23] Z. Xiang, "Discussion on: 'Integral sliding mode control for a class of uncertain switched nonlinear Systems,'" *Eur. J. Control*, vol. 16, no. 1, pp. 25–26, Jan. 2010.
- [24] J. X. Xu, "Discussion on: 'Integral sliding mode control for a class of uncertain switched nonlinear systems,'" *Eur. J. Control*, vol. 16, no. 1, pp. 23–25, 2010.

- [25] X. Zhang, "Robust integral sliding mode control for uncertain switched systems under arbitrary switching rules," *Nonlinear Anal., Hybrid Syst.*, vol. 37, Aug. 2020, Art. no. 100900.
- [26] M. Kchaou and S. Al Ahmadi, "Robust  $H_\infty$  control for nonlinear uncertain switched descriptor systems with time delay and nonlinear input: A sliding mode approach," *Complexity*, vol. 2017, pp. 1–14, Jun. 2017.
- [27] A. Ferrara, G. P. Incremona, and B. Sangiovanni, "Tracking control via switched integral sliding mode with application to robot manipulators," *Control Eng. Pract.*, vol. 90, pp. 257–266, Sep. 2019.
- [28] R. Galván-Guerra and L. Fridman, "Output integral sliding mode based robustified LQ control for switched uncertain systems," in *Proc. 13th Int. Workshop Variable Struct. Syst. (VSS)*, Jun. 2014, pp. 1–6.
- [29] R. Galván-Guerra, L. Fridman, J. E. Velázquez-Velázquez, S. Kamal, and B. Bandyopadhyay, "Continuous output integral sliding mode control for switched linear systems," *Nonlinear Anal., Hybrid Syst.*, vol. 22, pp. 284–305, Nov. 2016.
- [30] R. Galván-Guerra, L. Fridman, R. Iriarte, J.-E. Velázquez-Velázquez, and M. Steinberger, "Integral sliding-mode observation and control for switched uncertain linear time invariant systems: A robustifying strategy," *Asian J. Control*, vol. 20, no. 4, pp. 1551–1565, Jul. 2018.
- [31] J. E. Velázquez-Velázquez, R. Galván-Guerra, and L. Fridman, "Robust generation of self-oscillation in pendulum systems: A switched integral sliding mode control approach," *IFAC-PapersOnLine*, vol. 50, no. 1, pp. 7163–7168, 2017.
- [32] J.-E. Velázquez-Velázquez, R. Galván-Guerra, L. Fridman, and R. Iriarte, "Two relay control robustification by continuous switched integral sliding modes," *IET Control Theory Appl.*, vol. 13, no. 9, pp. 1374–1382, Jun. 2019.
- [33] X. Zhang, "Robust integral sliding mode control strategy under designed switching rules for uncertain switched linear systems via multiple Lyapunov functions," *Trans. Inst. Meas. Control*, vol. 41, no. 12, pp. 3536–3549, Aug. 2019.
- [34] T. Wang, L. Xie, and C. E. de Souza, "Robust control of a class of uncertain nonlinear systems," *Syst. Control Lett.*, vol. 19, no. 2, pp. 139–149, 1992.
- [35] R. A. Horn and C. R. Johnson, *Matrix Analysis*. Cambridge, U.K.: Cambridge Univ. Press, 2013.



**LINGFEI XIAO** received the Ph.D. degree from Zhejiang University, in 2008. She was a Visiting Scholar with the Department of Automatic Control and Systems Engineering, The University of Sheffield, U.K., in 2013. She is currently an Associate Professor with the Jiangsu Province Key Laboratory of Aerospace Power Systems, College of Energy and Power Engineering, Nanjing University of Aeronautics and Astronautics. Her main research interests include advanced control theory and application in complex mechanical and electrical systems, and aircraft engine systems.



**HAIFEN LI** was born in 1986. She received the B.S. degree from Northeast Petroleum University, in 2008, the M.S. degree in electrical engineering from the Tianjin University of Technology, Tianjin, China, in 2011, and the Ph.D. degree from Nankai University, in 2017. Since July 2017, she has been taught with the North China Institute of Science and Technology, where she is currently a Lecturer. Her research interests include modeling and dynamic filtering, and control of nonlinear systems.

• • •



**XIAOYU ZHANG** (Senior Member, IEEE) was born in 1978. He received the B.S. degree from Yanshan University, in 2000, and the M.S. and Ph.D. degrees from Zhejiang University, in 2003 and 2006, respectively.

From June 2006 to June 2007, he was with the School of Information Science and Engineering, Nanchang University. Since July 2007, he has been taught with the North China Institute of Science and Technology (NCIST), where he was an Associate Professor and a Professor. From 2018 to 2019, he was a Visiting Scholar with Columbia University, New York. He is currently a Professor with NCIST. His research interests include nonlinear control, intelligent control, switching systems, driving systems, power electronics, and complex systems.